

UNNS Substrate Research Program | Working Manuscript

Structural Realizability and Dual Observability in the Admissibility Manifold

A Second Structural Layer Between Admissibility and Dynamics

Instruments: STRUC-I v1.0.4 × STRUC-PERC-I v2.4.0

Corpus: 5,233 STRUC-I runs × 81 STRUC-PERC-I runs across 14 domains

Framework: Universal Structural Law · Percolative Realizability Principle

Status: Theorem-ready formulation — sufficient direction open

Date: 2026

Abstract

The Universal Structural Law (USL) establishes the admissible domain \mathcal{M}_{adm} of relational configurations through the inequality $\text{inv}(P_\varepsilon; L) \leq \nu(V_\varepsilon(L))$. Empirical evaluation by STRUC-I v1.0.4, across more than 1,500 ladders and ten physical domain families, produces zero hard violations at physical parameter values. We report here the results of a second, independent instrument—STRUC-PERC-I v2.4.0—applied to the same corpus across 81 runs and 14 domains, together with the theoretical consequences of the cross-instrument alignment.

STRUC-PERC-I evaluates the connectivity structure of the vulnerability graph $G_\kappa(L)$ of each ladder across scale κ , classifying each system by its *realizability class*: FULL, GIANT, TAIL, or HARD. The central finding is that admissibility (measured by structural pressure $\bar{\rho}$ and admissibility score A_κ^{min}) and realizability (measured by κ_{conn} and percolation tier) are *not reducible to one another*. Equal admissibility profiles can correspond to radically different realizability structures, and vice versa.

This non-reducibility is the primary empirical discovery: the admissibility manifold \mathcal{M}_{adm} possesses internal geometry—a realizability stratification—not captured by the admissibility coordinate $\bar{\rho}$ alone. We formalise this as a *Dual Observability Theorem* and derive five supporting results: a Non-Equivalence Theorem, a Coordinate Independence Theorem, a Realizability Refinement Theorem, a Forbidden State Theorem, and a Layered Structure Theorem. Together these elevate the Percolative Realizability Principle from a topological reformulation of the USL to a second structural layer lying strictly between admissibility and dynamics.

Cross-instrument analysis identifies five empirically distinct joint structural states—Relaxed-Connected, Moderate-Connected, Relaxed-Tail, Stressed-Extreme, and Stressed-Fragmented—replacing the two-state binary of either instrument in isolation. The Zeeman domain provides the sharpest example: $\bar{\rho} = 0.9585$ (CRITICAL zone, 4.15% margin to violation) with FULL percolation at $\kappa_{\text{conn}} = 2\text{--}4 \times 10^5$, demonstrating simultaneous maximum structural pressure and maximum connectivity delay. No physical system occupies the (high $\bar{\rho}$, HARD) cell of the joint matrix, empirically grounding the Forbidden State Theorem.

The paper closes with a formalisation of the structural hierarchy USL \rightarrow Admissibility \rightarrow Realizability \rightarrow Dynamics and identifies the open mathematical problems that the dual-layer theory generates.

Contents

1	Introduction	3
1.1	Background	3
1.2	The New Question	3
1.3	Main Results	3
1.4	Organisation	4
2	Setup and Notation	4
3	Realizability Structure	5
3.1	Scale Connectivity Profile	6
3.2	The Realizability Coordinate	6
4	Dual Observability	6
5	Non-Equivalence of Admissibility and Realizability	8
6	Coordinate Independence of Structural Observables	8
7	Realizability Refinement	9
8	The Joint Structural State	10
8.1	Five-State Taxonomy	10
9	The Forbidden State Theorem	11
10	The Layered Structure	12
11	Cross-Instrument Empirical Evidence	13
11.1	Corpus Summary	13
11.2	Domain-Level Cross-Instrument Results	13
11.3	The Zeeman Case: Coordinate Independence Sharpest Instance	13
11.4	The Nuclear Intra-Domain Discrimination	14
11.5	The Biological Case: Immediate Connectivity	14
11.6	Structural Phase Plane	15
11.7	Instrument Consistency and the TiO_2 Exception	16
12	Interpretive Consequences	16
12.1	Admissibility Is Necessary But Not Sufficient for Structural Organisation	16
12.2	Boundary Systems Are Dual-Tension States	17
12.3	Structural Regimes Require the Two-Component State	17
12.4	The Geometry of \mathcal{M}_{adm} Is Not Captured by Pressure Alone	17
13	Discussion and Open Questions	17
13.1	Relation to the PRP	17
13.2	The Sufficient Direction	18
13.3	Open Questions	18

14 Conclusion	19
14.1 What Has Been Established	19
14.2 What This Changes	19
14.3 The Central Shift	20
A Proof of the Dual Observability Theorem	20
A.1 Step 1: Logical Non-Reducibility	20
A.2 Step 2: Empirical Coordinate Independence	21
B Formal Derivation of the Realizability Classes	22
B.1 Vulnerability Graph (Foundation)	22
B.2 Giant Ratio and Dominant Backbone	22
B.3 Derivation of the Four Classes	23
B.4 Exhaustiveness and Mutual Exclusivity	23
B.5 Link to Dual Observability	24

1 Introduction

1.1 Background

The Universal Structural Law (USL) asserts that every persistent ordered physical sequence—every ladder L —satisfies the admissibility inequality

$$\text{inv}(P_\varepsilon; L) \leq \nu(V_\varepsilon(L)), \quad (1)$$

where $\text{inv}(P_\varepsilon; L)$ counts inversions in the ε -persistence set and $\nu(V_\varepsilon(L))$ is the admissible inversion capacity. Empirical evaluation via STRUC-I v1.0.4 across more than 1,500 ladders and ten physical domain families has produced zero hard violations at physical parameter values [1], a result robust to constant deformations spanning the fine-structure constant α , the proton-to-electron mass ratio μ , the strong coupling α_s , and the gravitational coupling α_G .

The Foundations document [1] also establishes that admissible configurations are not uniformly distributed within \mathcal{M}_{adm} . They occupy a structured landscape characterised by structural pressure $\bar{\rho}$, admissibility score A_κ^{min} , and a four-regime taxonomy (Ultra-Stable Interior, Weak Persistence, Boundary-Stabilised, Boundary-Adjacent). This is the geometry of admissibility: a first-order coordinate system on \mathcal{M}_{adm} .

The Percolative Realizability Principle (PRP) [2] provides a topological reformulation of the same admissibility condition in terms of the connectivity of the vulnerability graph $G_\kappa(L)$. It identifies a necessary direction—severe (HARD-class) fragmentation implies the existence of a deformation inducing a USL violation.

1.2 The New Question

Neither the Foundations document nor the PRP raises the following question:

Do admissibility (the inversion-pressure coordinate of STRUC-I) and realizability (the connectivity coordinate of STRUC-PERC-I) measure the same structural property, or independent properties?

This is not a question about whether the two instruments agree or disagree on which systems are admissible. It is a question about the *internal geometry* of \mathcal{M}_{adm} : whether the structural state of an admissible configuration is fully described by $\bar{\rho}$ alone, or whether it requires an additional coordinate.

The empirical answer, established in this paper via cross-instrument analysis of 81 STRUC-PERC-I runs across 14 domains matched against 5,233 STRUC-I runs, is unambiguous: the two instruments measure independent structural properties. Equal admissibility does not imply equal realizability. Equal realizability does not imply equal admissibility. The two coordinates are empirically independent on \mathcal{M}_{adm} .

1.3 Main Results

The paper establishes the following:

1. **Dual Observability Theorem** (Section 4): every admissible configuration $S \in \mathcal{M}_{\text{adm}}$ admits two independent observable projections—admissibility pressure and realizability connectivity—that are not reducible to each other.
2. **Non-Equivalence Theorem** (Section 5): there exist admissible configurations S_1, S_2 with $\bar{\rho}(S_1) = \bar{\rho}(S_2)$ but $\mathcal{R}(S_1) \neq \mathcal{R}(S_2)$.
3. **Coordinate Independence Theorem** (Section 6): admissibility and realizability define independent coordinates on \mathcal{M}_{adm} ; neither coordinate function determines the other.
4. **Realizability Refinement Theorem** (Section 7): realizability induces a strictly finer partition of \mathcal{M}_{adm} than admissibility alone.
5. **Forbidden State Theorem** (Section 9): no observed physical configuration simultaneously satisfies $\bar{\rho} \rightarrow 1$ and $\mathcal{R} = \text{HARD}$.
6. **Layered Structure Theorem** (Section 10): the structural description of physical systems admits a strict hierarchy: USL \rightarrow Admissibility \rightarrow Realizability \rightarrow Dynamics.

1.4 Organisation

Section 2 fixes notation. Section 3 develops the realizability structure. Sections 4–10 state and prove the six main results. Section 11 presents the cross-instrument empirical evidence. Section 8 introduces the joint structural state and five-state taxonomy. Section 12 derives interpretive consequences. Section 13 discusses open questions. Section 14 concludes.

Central Theorem (Structural Duality). *Structural configurations in \mathcal{M}_{adm} require two independent coordinates for a complete description: the admissibility coordinate $(\bar{\rho}, A_{\kappa}^{\min})$, measuring constraint proximity to the USL boundary, and the realizability coordinate $(\mathcal{C}, \kappa_{\text{conn}})$, measuring internal gap-graph connectivity. Neither coordinate determines the other. Together they define the structural state $\mathcal{S}(S) = (\bar{\rho}(S), \mathcal{R}(S))$ of every admissible configuration.*

Informal consequence: Admissibility answers whether a structure can exist. Realizability answers how it exists.

2 Setup and Notation

We adopt the notation of the Foundations document [1] and the PRP paper [2]. A *ladder* is a finite weakly ordered sequence $L = (x_1 \leq x_2 \leq \dots \leq x_n)$ with gap vector $\Delta = (\Delta_i)_{i=1}^{n-1}$ where $\Delta_i = x_{i+1} - x_i \geq 0$ and median gap $\tilde{\Delta} = \text{median}(\Delta)$.

Definition 2.1 (Deformation parameters). Fix $\kappa \in (0, 1]$ and set $\varepsilon = \kappa \cdot \tilde{\Delta}$. The scale domain $\mathcal{K} = \{\kappa_1 < \dots < \kappa_m\}$ is a 17-point grid in the STRUC-I protocol and a 40-point grid with Monte Carlo sampling in the STRUC-PERC-I protocol.

Definition 2.2 (Admissibility score and structural pressure). The admissibility score at scale κ is $A_\kappa(L) = \text{inv}(P_\varepsilon; L) / \nu(V_\varepsilon(L)) \in [0, 1]$. The *structural pressure* of L is

$$\bar{\rho}(L) = \frac{1}{|\mathcal{K}|} \sum_{\kappa \in \mathcal{K}} A_\kappa(L).$$

A ladder is admissible if $A_\kappa(L) \leq 1$ for all $\kappa \in \mathcal{K}$; a hard violation occurs when $A_\kappa(L) < A_{\text{thresh}} = 0.52$ for some κ .

Definition 2.3 (Vulnerability graph and realizability). For a ladder L and scale κ , the *vulnerability graph* $G_\kappa(L) = (V, E_\kappa)$ has vertex set $V = \{1, \dots, n-1\}$ indexing the gaps of L and edge set

$$(i, j) \in E_\kappa \iff |\Delta_i - \Delta_j| \leq \varepsilon = \kappa \tilde{\Delta}.$$

The connected components of $G_\kappa(L)$ define the *realizability structure* of L at scale κ .

Definition 2.4 (Percolation chain). A ladder L *admits a percolation chain* if there exists a sequence of connected components $\{C_\kappa\}_{\kappa \in \mathcal{K}}$ in $\{G_\kappa(L)\}_{\kappa \in \mathcal{K}}$ such that: (i) consecutive components intersect (strict continuity across scales), and (ii) the union spans all vertices V at κ_{max} .

Definition 2.5 (Realizability class). A ladder L is assigned a realizability class from the following ordered tier system:

- FULL: complete connectivity $|C_{\kappa_{\text{max}}}| = |V|$ achieved.
- GIANT: near-complete connectivity; the largest component contains $\geq 90\%$ of vertices; a tail of isolated vertices persists.
- TAIL: a large-variance isolated component persists; global connectivity is not achieved within the tested κ -range.
- HARD: persistent multi-component fragmentation with no scale-continuous connected component, for which a deformation exists inducing a USL violation (PRP Theorem 1).

The *connectivity threshold* κ_{conn} is the smallest κ at which the FULL or GIANT verdict is first achieved; it is undefined ($\kappa_{\text{conn}} = \infty$) for TAIL and HARD.

Definition 2.6 (Admissibility manifold). Following [1], the admissibility manifold is

$$\mathcal{M}_{\text{adm}} = \{S \in \mathcal{S} \mid A_\kappa(S, c) \leq 1 \forall \kappa \in \mathcal{K}, \forall c \in C\},$$

where \mathcal{S} is the space of all formally constructible configurations and C is the admissible deformation domain. The selection operator $\Sigma : \mathcal{S} \rightarrow \{0, 1\}$ is defined by $\Sigma(S) = 1 \iff S \in \mathcal{M}_{\text{adm}}$.

3 Realizability Structure

The realizability structure of an admissible configuration is defined by the multi-scale behaviour of its vulnerability graph.

3.1 Scale Connectivity Profile

Definition 3.1 (Connectivity profile). For $L \in \mathcal{M}_{\text{adm}}$, the *connectivity profile* of L is the function

$$\Pi_L : \mathcal{K} \longrightarrow \mathbb{Z}_{\geq 0} \times \mathbb{R}, \quad \Pi_L(\kappa) = (|V/G_\kappa(L)|, \text{GR}(\kappa)),$$

where $|V/G_\kappa(L)|$ is the number of connected components of $G_\kappa(L)$ and $\text{GR}(\kappa) = \max_C |C|/|V|$ is the giant ratio (fraction of vertices in the largest component).

Definition 3.2 (Tail dominance). The *tail dominance* of L at scale κ is the ratio of the maximum gap to the IQR of the gap distribution, scaled by κ . A ladder is *tail-dominated* at κ if one or more gaps are outliers relative to the bulk distribution at that scale. Tail dominance governs whether a single extreme transition delays global connectivity.

Remark 3.3. In the nuclear domain, tail-dominated ladders arise from single extreme-energy γ -transitions (e.g. in ^{238}U and ^{48}Ca) that lie orders of magnitude above the bulk spectral spacing. In the Zeeman domain, fine-structure transitions constitute the outlier set. The physical mechanism differs; the structural signature—delayed percolation with high tail dominance—is common.

3.2 The Realizability Coordinate

Definition 3.4 (Realizability coordinate). The *realizability coordinate* of an admissible configuration $S \in \mathcal{M}_{\text{adm}}$ is the pair

$$\mathcal{R}(S) = (\mathcal{C}(S), \kappa_{\text{conn}}(S)),$$

where $\mathcal{C}(S) \in \{\text{FULL}, \text{GIANT}, \text{TAIL}, \text{HARD}\}$ is the realizability class and $\kappa_{\text{conn}}(S)$ is the connectivity threshold (Definition 2.5).

Remark 3.5. The realizability coordinate $\mathcal{R}(S)$ is independent of the admissibility coordinate $(\bar{\rho}(S), A_\kappa^{\text{min}}(S))$ in the sense made precise by Theorem 6.1: neither coordinate determines the other within the physically observed corpus.

Remark 3.6 (Instrument-relativity of realizability). The realizability coordinate as defined here is *instrument-relative*: it depends on the specific edge predicate $|\Delta_i - \Delta_j| \leq \kappa \tilde{\Delta}$ and the IQR-scaled ε of STRUC-PERC-I v2.4.0. A different threshold function or a different graph construction could yield a different connectivity profile. Establishing that the realizability class $\mathcal{C}(S)$ and threshold $\kappa_{\text{conn}}(S)$ are invariant under alternative admissible constructions is an open problem. The empirical findings reported here are specific to the STRUC-PERC-I protocol; their structural interpretation is conjectured to be robust, but this robustness has not yet been formally established.

4 Dual Observability

Theorem 4.1 (Dual Observability Theorem). *Every admissible configuration $S \in \mathcal{M}_{\text{adm}}$ admits two independent observable projections:*

1. Admissibility projection: $A_\kappa(S, c) \leq 1$ — *structural pressure and budget usage.*

2. Realizability projection: *the connectivity structure of $G_\kappa(L)$ across scales — percolation class and connectivity delay.*

These projections are not reducible to one another.

Proof. We prove independence in two steps: (i) logical non-reducibility (the projections are defined on mathematically distinct objects), and (ii) empirical coordinate independence (no functional relation holds in the observed corpus). The full derivation is given in Appendix A; we state the structure here.

Step 1: Logical non-reducibility. The admissibility projection is a global combinatorial count on the ε -persistence set $P_\varepsilon(L)$: the scalars $\bar{\rho}(S)$ and $A_\kappa^{\min}(S)$ depend only on the number of order-inverting pairs $\text{inv}(P_\varepsilon; L)$ and the variation capacity $\nu(V_\varepsilon(L))$.

The realizability projection is a topological property of the vulnerability graph $G_\kappa(L) = (V, E_\kappa)$ with vertices indexing gaps $\Delta_i = x_{i+1} - x_i$ and edges $(i, j) \in E_\kappa \iff |\Delta_i - \Delta_j| \leq \varepsilon$. The class $\mathcal{C}(S) \in \{\text{FULL}, \text{GIANT}, \text{TAIL}, \text{HARD}\}$ and threshold $\kappa_{\text{conn}}(S)$ are connected-component invariants of this graph.

There is no algebraic identity equating the inversion-count scalars $\bar{\rho}$, A_κ^{\min} with the graph-connectivity invariants \mathcal{C} , κ_{conn} : the former depend only on the number of inverting pairs; the latter depend on the connected components of the gap-distance graph. Hence the projections are logically distinct; independence is then established empirically in Step 2.

Step 2: Empirical coordinate independence. The cross-instrument corpus (5,233 STRUC-I \times 81 STRUC-PERC-I runs, 10 shared domains) provides explicit counterexamples showing equal $\bar{\rho}$ with different \mathcal{C} , and equal \mathcal{C} with widely varying $\bar{\rho}$.

Counterexample set 1 (equal $\bar{\rho}$, different realizability). Nuclear domain (ENSDF, 14 isotopes): $\bar{\rho} \approx 0.197$ (RELAXED zone). Ten isotopes: FULL at $\kappa_{\text{conn}} = 3.8 \times 10^4 - 4.2 \times 10^5$. Four isotopes (^{48}Ca , ^{100}Mo , ^{150}Nd , ^{238}U): TAIL (tail dominance = 1.000, gap ratios up to 2×10^{18}). Molecular domain (HITRAN): $\bar{\rho} = 0.103$ (also RELAXED) \rightarrow GIANT with no κ_{conn} . Thus $\bar{\rho} \approx 0.10 - 0.20$ spans FULL, TAIL, and GIANT.

Counterexample set 2 (overlapping $\bar{\rho}$, extreme realizability difference). Biological domain (QT45 ribozyme): $\bar{\rho} \in [0.188, 0.819] \rightarrow$ FULL at $\kappa_{\text{conn}} = 0.42 - 2.00$ (lowest in corpus). Nuclear domain at comparable $\bar{\rho} \approx 0.19 - 0.30$: FULL/TAIL at $\kappa_{\text{conn}} \sim 10^4 - 10^5$. Factor $10^4 - 10^5$ difference in κ_{conn} at overlapping pressure.

Counterexample set 3 (same realizability class, wide $\bar{\rho}$ range). FULL class spans $\bar{\rho} = 0.086$ (atmosphere, ERA5) to $\bar{\rho} = 0.9585$ (Zeeman). GIANT class spans $\bar{\rho} = 0.103$ (molecular) to $\bar{\rho} \approx 0.65$ (cosmic web peak). TAIL class appears at both low and elevated pressure.

Sharpest single instance — Zeeman domain. $\bar{\rho} = 0.9585 \pm 0.00004$ (CRITICAL zone, 4.15% margin) combined with FULL at $\kappa_{\text{conn}} = 2 - 4 \times 10^5$ (extreme delay). Maximum inversion pressure and maximum connectivity delay coexist; neither measurement predicts the other.

Since the corpus contains configurations with identical $\bar{\rho}$ but different \mathcal{C} (and vice versa), and no functional relation $\mathcal{R} = f(\bar{\rho})$ or $\bar{\rho} = g(\mathcal{R})$ holds, the coordinates are empirically independent.

Conclusion. The projections are logically distinct (Step 1) and empirically non-reducible (Step 2). Therefore every admissible configuration S requires the two-component structural state $\mathcal{S}(S) = (\bar{\rho}(S), \mathcal{R}(S))$ for complete characterisation. \square

Corollary 4.2. *A complete structural characterisation of a configuration $S \in \mathcal{M}_{\text{adm}}$ requires both the admissibility projection $(\bar{\rho}, A_{\kappa}^{\text{min}})$ and the realizability projection $\mathcal{R}(S)$. Neither suffices alone.*

5 Non-Equivalence of Admissibility and Realizability

Theorem 5.1 (Non-Equivalence Theorem). *There exist admissible configurations $S_1, S_2 \in \mathcal{M}_{\text{adm}}$ such that*

$$\bar{\rho}(S_1) = \bar{\rho}(S_2) \quad \text{but} \quad \mathcal{R}(S_1) \neq \mathcal{R}(S_2),$$

where \mathcal{R} denotes the realizability coordinate of Definition 3.4.

Proof sketch. Three independent empirical instances are observed in the cross-instrument corpus.

Instance 1: Nuclear versus molecular pressure zone. The nuclear corpus (ENSDF, 14 isotopes) returns a corpus-averaged structural pressure $\bar{\rho} = 0.197$ (RELAXED zone), identical in zone classification to the molecular corpus (HITRAN, $\bar{\rho} = 0.103$, also RELAXED). Yet realizability differs categorically: molecular ladders classify as GIANT with no κ_{conn} (connectivity threshold not reached in tested range), while nuclear FULL ladders achieve connectivity at $\kappa_{\text{conn}} = 3.8 \times 10^4$ – 4.2×10^5 —four to five orders of magnitude larger.

Instance 2: Nuclear FULL versus TAIL at equal pressure. Within the nuclear corpus, isotopes ^{24}Mg – ^{48}Ti (FULL, $\bar{\rho} \approx 0.20$) and ^{48}Ca , ^{100}Mo , ^{150}Nd , ^{238}U (TAIL, comparable $\bar{\rho}$) share structural pressure zones yet differ in realizability class. The TAIL isotopes exhibit tail dominance = 1.000 with extreme gap ratios up to 2×10^{18} , driven by single anomalous γ -transitions. Equal $\bar{\rho}$ does not predict TAIL versus FULL.

Instance 3: Biological versus nuclear at overlapping pressure. The biological corpus (QT45 ribozyme fitness landscape, $\bar{\rho} \in [0.188, 0.819]$) overlaps the nuclear pressure range in its lower values. At $\bar{\rho} \approx 0.20$, nuclear ladders achieve connectivity at $\kappa_{\text{conn}} \approx 10^5$ while biological ladders achieve connectivity at $\kappa_{\text{conn}} = 0.42$ – 2.00 —a factor of 10^5 difference in connectivity threshold at comparable admissibility pressure.

In all three instances, equal or overlapping $\bar{\rho}$ does not determine equal realizability class or κ_{conn} . Therefore the realizability coordinate is not determined by the admissibility coordinate, and the two are non-equivalent. \square

Remark 5.2. Instance 3 is particularly striking. The factor- 10^5 difference in κ_{conn} between biological and nuclear ladders at comparable $\bar{\rho}$ reflects the gap homogeneity of fitness landscapes versus the extreme-energy tail structure of nuclear γ -spectra. Both are admissible, both in the RELAXED–STABLE pressure range; their internal gap organisations are categorically different.

6 Coordinate Independence of Structural Observables

Theorem 6.1 (Coordinate Independence Theorem). *Admissibility and realizability define independent coordinates on \mathcal{M}_{adm} :*

$$\mathcal{S}(S) = (\bar{\rho}(S), \mathcal{R}(S)),$$

such that neither coordinate function determines the other.

Proof sketch. From Theorem 5.1, realizability varies at fixed $\bar{\rho}$ (Instances 1–3). It remains to show that $\bar{\rho}$ varies at fixed realizability class.

Within the FULL realizability class, the corpus spans: $\bar{\rho} = 0.086$ (atmosphere, ERA5) to $\bar{\rho} = 0.9585$ (Zeeman), a factor of 11 variation. Within GIANT: $\bar{\rho} = 0.103$ (molecular) to $\bar{\rho} \approx 0.65$ (cosmic web peak). Within TAIL: comparable variation across the nuclear TAIL isotopes and the upper biological range.

In each realizability class, the admissibility pressure varies continuously and substantially. No realizability class is confined to a narrow pressure band.

Therefore, the two coordinates are empirically independent: neither determines the other within the observed corpus, and the pair $(\bar{\rho}, \mathcal{R})$ provides a non-redundant two-component description of admissible configurations.

The Zeeman domain makes this independence most visible. Its STRUC-I measurement ($\bar{\rho} = 0.9585$, CRITICAL zone, $A_{\kappa}^{\min} = 0.9990$, 4.15% margin) places it at the extreme of the admissibility axis. Its STRUC-PERC-I measurement (FULL at $\kappa_{\text{conn}} = 2\text{--}4 \times 10^5$) places it at the extreme of the connectivity delay axis. The system is simultaneously at the boundary from the inversion direction and fully connected from the percolation direction. This is not a contradiction; it is the signature of two empirically independent structural observables. \square

Remark 6.2 (Empirical coordinate independence). The independence established here is *empirical coordinate independence*, not formal geometric orthogonality: no metric tensor or inner product is yet defined on \mathcal{M}_{adm} relative to which the two coordinates are orthogonal in the Euclidean sense. What is established is that \mathcal{M}_{adm} admits at least a two-dimensional coordinate chart in $(\bar{\rho}, \mathcal{R})$, and that no functional relation between the coordinates is observed in the tested corpus. A formal geometric structure incorporating both coordinates is an open problem (Section 13).

7 Realizability Refinement

Theorem 7.1 (Realizability Refinement Theorem). *Realizability induces a strictly finer partition of \mathcal{M}_{adm} than admissibility alone.*

Proof sketch. The admissibility coordinate $\bar{\rho}$ partitions \mathcal{M}_{adm} into four pressure zones: STABLE ($\bar{\rho} < 0.3$), WEAK PERSISTENCE ($0.3 \leq \bar{\rho} < 0.6$), CRITICAL ($0.6 \leq \bar{\rho} < 0.9$), and BOUNDARY ($\bar{\rho} \geq 0.9$). The realizability coordinate independently partitions \mathcal{M}_{adm} into four tier classes: FULL, GIANT, TAIL, HARD.

Since the two partitions are based on independent coordinates (Theorem 6.1), their product partition is strictly finer than either alone. Explicitly: the STABLE zone contains both FULL and GIANT ladders (e.g. biological FULL at low $\bar{\rho}$, and molecular GIANT at low $\bar{\rho}$); the RELAXED zone contains FULL, TAIL, and GIANT (nuclear FULL, nuclear TAIL, molecular GIANT); the CRITICAL zone contains FULL (Zeeman at extreme κ_{conn}) and GIANT/TAIL (atomic normal spectra); and the BOUNDARY zone contains only FULL in the current corpus but is not logically restricted to it.

Therefore, the joint classification (pressure zone, \mathcal{C}) is strictly finer than either component alone, and realizability is a non-trivial refinement of the admissibility partition. \square

Corollary 7.2. *The TYPE classification system of [1] (TYPE I, II, III variants based on $\bar{\rho}$ and A_{κ}^{\min} trajectories) does not distinguish between systems with identical admissibility profiles but different realizability structures. Incorporating the realizability coordinate \mathcal{R} yields a strictly more discriminating classification.*

Example 7.3. Within the nuclear corpus under the α_s column, ^{208}Pb and ^{48}Ca are both classified TYPE I-calm and TYPE III-Fr respectively by STRUC-I, reflecting their differing admissibility trajectories. STRUC-PERC-I reveals an additional distinction: ^{208}Pb (doubly magic, closed shells) achieves connectivity at $\kappa_{\text{conn}} \approx 3.8 \times 10^4$, while ^{48}Ca and ^{150}Nd classify as TAIL with tail dominance 1.000—a finding invisible to STRUC-I alone.

8 The Joint Structural State

Definition 8.1 (Structural state). The *structural state* of a configuration $S \in \mathcal{M}_{\text{adm}}$ is the pair

$$\mathcal{S}(S) = (\bar{\rho}(S), \mathcal{R}(S)).$$

Remark 8.2. The structural state replaces the scalar admissibility metric $\bar{\rho}$ with a two-component description capturing both constraint (how much of the admissibility budget is used) and organisation (how the gap structure is connected at each scale). The admissibility manifold \mathcal{M}_{adm} therefore admits at least a two-dimensional coordinate chart in $(\bar{\rho}, \mathcal{R})$, not a one-dimensional interval in $\bar{\rho}$. Whether this chart extends to a full product structure $\mathcal{M}_{\text{adm}} \cong [\rho_{\min}, 1] \times \mathcal{R}$ is an open mathematical question.

8.1 Five-State Taxonomy

Cross-instrument analysis of the shared corpus identifies five empirically distinct structural states. These are not imposed classification bins; they are natural clusters in the $(\bar{\rho}, \mathcal{C}, \kappa_{\text{conn}})$ space observed across the 10 shared domains. The taxonomy presented here is a *first-order empirical atlas*, not an exhaustive or provably complete classification: future domains or finer instrument resolution may reveal additional states or split existing ones. It replaces the two-state binary of either instrument in isolation.

Definition 8.3 (Joint structural taxonomy). The five empirically observed joint structural states are:

1. **Relaxed-Connected** ($\bar{\rho} < 0.3$, FULL or GIANT, $\kappa_{\text{conn}} \leq 2$): low admissibility pressure with immediate or rapid connectivity. *Exemplars:* biological fitness landscapes ($\bar{\rho} = 0.188\text{--}0.819$, $\kappa_{\text{conn}} = 0.42\text{--}2.00$), atmospheric ladders (ERA5, $\bar{\rho} = 0.086\text{--}0.225$, $\kappa_{\text{conn}} = 0.42\text{--}2.00$).
2. **Moderate-Connected** ($\bar{\rho} = 0.15\text{--}0.30$, FULL, κ_{conn} moderate): intermediate pressure with achieved connectivity at moderate delay. *Exemplars:* nuclear FULL isotopes ($\bar{\rho} = 0.197$, $\kappa_{\text{conn}} = 3.8 \times 10^4\text{--}4.2 \times 10^5$), condensed matter FULL ($\bar{\rho} = 0.178\text{--}0.263$, $\kappa_{\text{conn}} = 0.75\text{--}8072$).
3. **Relaxed-Tail** ($\bar{\rho} < 0.3$, GIANT or TAIL, no κ_{conn}): low admissibility pressure with persistent tail fragmentation; global connectivity not achieved in tested range. *Exemplars:* molecular ladders (HITRAN, $\bar{\rho} = 0.103$, GIANT), geoid harmonics (TYPE I Tier A), cosmic web at typical $\bar{\rho}$ (GIANT/TAIL).

4. **Stressed-Extreme** ($\bar{\rho} \geq 0.9$, FULL, $\kappa_{\text{conn}} \gg 1$): extreme admissibility pressure with full connectivity achieved only at anomalously large scale. *Exemplar*: Zeeman domain ($\bar{\rho} = 0.9585$, FULL at $\kappa_{\text{conn}} = 2\text{--}4 \times 10^5$).
5. **Stressed-Fragmented** ($\bar{\rho}$ elevated, TAIL, no κ_{conn}): elevated pressure with persistent fragmentation; global connectivity not achieved. *Exemplars*: cosmic web at peak density ($\bar{\rho} = 0.651$, TAIL), solar flare ladders.

Proposition 8.4. *The five-state taxonomy is strictly more informative than the admissibility taxonomy of [1] or the realizability taxonomy of [2] in isolation: it discriminates systems that each taxonomy treats as equivalent.*

Proof sketch. The admissibility taxonomy groups nuclear ($\bar{\rho} = 0.197$, RELAXED) and molecular ($\bar{\rho} = 0.103$, RELAXED) in the same zone; the five-state taxonomy separates them into Moderate-Connected and Relaxed-Tail. The realizability taxonomy groups biological and atmospheric ladders (both FULL at low κ_{conn}) with condensed matter (FULL at moderate κ_{conn}); the five-state taxonomy separates them by pressure zone. In each case, the joint taxonomy resolves a degeneracy. \square

9 The Forbidden State Theorem

Theorem 9.1 (Forbidden State Theorem). *No observed physical configuration simultaneously satisfies*

$$\bar{\rho} \rightarrow 1 \quad \text{and} \quad \mathcal{C}(S) = \text{HARD}.$$

Proof sketch. Across the shared corpus (81 STRUC-PERC-I runs, 10 shared domains), the single HARD_FRAGMENTATION verdict arises for the TiO_2 raw density-of-states ladder (condensed matter domain, giant ratio $\text{GR} = 0.833$, below the FULL/GIANT threshold). This ladder has $\bar{\rho} = 0.033$ (STABLE zone)—extreme low pressure, not high. It does not represent the physical TiO_2 crystal phase chain (which yields $\bar{\rho} = 0.033$, FULL at $\kappa_{\text{conn}} = 681$) but rather the raw density-of-states representation, which STRUC-I does not evaluate. The HARD result is therefore a representation-sensitivity finding, not a physical system in the HARD class.

No physical system in the CRITICAL or BOUNDARY admissibility zone ($\bar{\rho} \geq 0.6$) exhibits HARD fragmentation. The Zeeman domain, with $\bar{\rho} = 0.9585$ (the highest pressure in the corpus), achieves FULL percolation at extreme κ_{conn} . High-pressure domains in the corpus (nuclear boundary-stabilised, Zeeman, atomic normal) are either FULL or TAIL, never HARD.

Interpretation: The observed pattern *suggests* a structural incompatibility between high inversion pressure and persistent fragmentation. A system under extreme inversion pressure ($\bar{\rho} \rightarrow 1$) has a gap structure in which a large fraction of gap pairs are within ε of one another at some scale κ , which is also the condition favouring broad connectivity in $G_\kappa(L)$. Persistent fragmentation (HARD) requires isolated components that resist merging across the full scale range, a condition that appears in tension with the dense gap clustering implied by high $\bar{\rho}$. The observed absence of the (high $\bar{\rho}$, HARD) state is consistent with this structural tension, but the corpus-relative nature of the theorem prevents a stronger claim. \square

Remark 9.2. The Forbidden State Theorem is corpus-relative: it asserts empirical exclusion within the tested domains, not logical impossibility. A single confirmed physical system with $\bar{\rho} \geq 0.8$ and $\mathcal{C} = \text{HARD}$ would refute it. The theorem is falsifiable.

Corollary 9.3. *Boundary-adjacent admissible configurations (those with $\bar{\rho} \geq 0.8$ in the current corpus) are constrained to the Stressed-Extreme or Stressed-Fragmented states. HARD fragmentation is excluded at high pressure.*

10 The Layered Structure

Theorem 10.1 (Layered Structure Theorem). *The structural description of physical systems admits a strict hierarchy:*

1. USL (constraint): $A_\kappa(S, c) \leq 1$ for all κ, c .
2. Admissibility (Σ filter): defines \mathcal{M}_{adm} as the domain of structural persistence.
3. Realizability (connectivity): defines the internal organisation of \mathcal{M}_{adm} via the gap graph $G_\kappa(L)$.
4. Dynamics: describes the behaviour of persistent configurations.

Each level presupposes the one above it. No level is reducible to any other.

Proof sketch. The four levels are defined by distinct objects:

- Level 1 (USL): the inequality $\text{inv}(P_\varepsilon; L) \leq \nu(V_\varepsilon(L))$ — a global constraint on counting functions.
- Level 2 (Admissibility): the set $\mathcal{M}_{\text{adm}} = \Sigma^{-1}(1)$ — a structural manifold defined by the inequality.
- Level 3 (Realizability): the connectivity of $G_\kappa(L)$ across scales — a topological property of the gap graph, defined *within* \mathcal{M}_{adm} .
- Level 4 (Dynamics): physical laws governing evolution, conservation, and symmetry of persistent configurations.

Presupposition chain: Admissibility requires the USL (it is defined by the inequality). Realizability requires admissibility: the connectivity of $G_\kappa(L)$ is a property of admissible configurations; it is not meaningful to classify the percolation tier of a ladder that violates the USL. Dynamics requires structural persistence: physical laws operate on configurations already satisfying the admissibility condition ([1], Theorem 5.6).

Non-reducibility: Level 2 does not determine Level 3 (Theorem 5.1). Level 3 does not determine Level 2 (Theorem 6.1). Neither determines Level 4: the dynamical laws governing H_2 , a nuclear isotope, and a ribozyme are entirely distinct, yet all satisfy Levels 1–3. \square

Corollary 10.2 (Percolative Realizability Layer). *Realizability defines a structural layer between admissibility and dynamics. Admissibility determines which configurations can persist; realizability determines how admissible configurations are internally connected. Dynamics describes what happens among configurations that are already persistent and connected.*

Proposition 10.3 (Complementarity of USL and PRP). *The USL and the Percolative Realizability Principle are complementary:*

- *USL \rightarrow bounds structural capacity (inversion budget).*
- *PRP \rightarrow organises that capacity (gap-graph connectivity).*

Neither principle reduces to the other; together they form the dual-layer theory.

11 Cross-Instrument Empirical Evidence

This section presents the empirical basis for the theorems of Sections 4–10, drawn from the cross-instrument corpus: 5,233 STRUC-I runs and 81 STRUC-PERC-I runs across 10 shared domains.

11.1 Corpus Summary

Table 1: STRUC-PERC-I v2.4.0 corpus summary: 81 runs across 14 domains.

Verdict class	Count	Metric	Value
FULL percolation	48	USL hard violations	0
GIANT component	23	Theorem 1 (PRP) triggered	1 / 81
TAIL fragmentation	9	Conjecture 1 (PRP)	open
HARD fragmentation	1	Shared domains (cross-instrument)	10
Total	81	Physical contradictions	0

11.2 Domain-Level Cross-Instrument Results

Table 2: Cross-instrument corpus: admissibility (STRUC-I) versus realizability (STRUC-PERC-I) by domain. $\bar{\rho}$: structural pressure. A^{\min} : minimum admissibility score. \mathcal{C} : realizability class. GR: giant ratio. κ_{conn} : connectivity threshold; “–” = not achieved in tested range.

Domain	$\bar{\rho}$	Zone	A^{\min}	\mathcal{C}	GR	κ_{conn}
Atomic / Zeeman	0.9585	CRITICAL	0.9990	FULL	1.0000	$2\text{--}4 \times 10^5$
Atomic / Normal	0.21–0.66	TENSION	1.0000	FULL/TAIL	0.994–1.00	$2\text{--}4 \times 10^5$
Biological (QT45)	0.188–0.819	STABLE \rightarrow BDY	≈ 1.000	FULL	1.0000	0.42–2.00
Nuclear (ENSDF)	0.197	RELAXED	1.0000	FULL/TAIL	0.976–1.00	$3.8\text{--}420 \times 10^3$
Condensed Matter	0.178–0.263	STABLE–WEAK	0.9995	FULL/HARD	0.833–1.00	0.75–8072
CMB (Planck 2018)	—	(not in SI)	—	FULL	1.0000	230–2389
Cosmic Web	0.143 (pk 0.651)	STABLE–WEAK	≈ 1.000	GIANT/TAIL	0.994–0.999	—
Atmosphere (ERA5)	0.086–0.225	RELAX–STABLE	≈ 1.000	FULL	1.0000	0.42–2.00
Molecular (HITRAN)	0.103	RELAXED	1.0000	GIANT	0.9985	—
Geodesy / GPS	—	(not in SI)	—	FULL/GIANT	0.999	—

11.3 The Zeeman Case: Coordinate Independence Sharpest Instance

The Zeeman domain (Stark-split and Zeeman-split atomic spectral ladders from Li to Au) represents the clearest single demonstration of the Dual Observability Theorem.

STRUC-I measurement. $\bar{\rho} = 0.9585 \pm 0.00004$ (across all Zeeman variants from H to Au), placing the Zeeman domain in the CRITICAL admissibility zone with a margin of only 4.15% before hard violation. This is the highest structural pressure in the entire physical corpus.

STRUC-PERC-I measurement. FULL percolation at $\kappa_{\text{conn}} = 2\text{--}4 \times 10^5$ —the most extreme connectivity delay of any domain. The gap structure divides into a dense bulk of nearly-equal fine-structure splittings and a handful of anomalously large hyperfine transitions; the bulk connects immediately but the tail transitions delay global integration to extreme κ_{conn} .

Interpretation. The Zeeman domain is simultaneously at maximum structural pressure (STRUC-I) and at maximum connectivity delay (STRUC-PERC-I). Neither measurement predicts the other. Both are required to characterise the boundary-stabilised state. The physical mechanism is the same in both cases—fine-structure splittings dominate the bulk, hyperfine transitions constitute the outliers—but the mechanism appears as high inversion pressure in one projection and as high connectivity delay in the other. This is the operational signature of two empirically independent structural observables.

11.4 The Nuclear Intra-Domain Discrimination

Within the nuclear corpus, 10 isotopes classify as FULL and 4 as TAIL (Table 3). The TAIL isotopes are ^{238}U , ^{150}Nd , ^{100}Mo , and ^{48}Ca —all with known structural anomalies: deformed nuclei, shape coexistence, or collectivity transitions. Their tail dominance is 1.000 with gap ratios reaching 2×10^{18} .

Table 3: Nuclear corpus (ENSDF): STRUC-PERC-I classification. “Tail dom.”: tail dominance ratio.

Isotope	Verdict	GR	Tail dom.
$^{24}\text{Mg} - ^{48}\text{Ti}$ (10 isotopes)	FULL	0.976–1.000	moderate
^{48}Ca	TAIL	< 0.98	1.000
^{100}Mo	TAIL	< 0.98	1.000
^{150}Nd	TAIL	< 0.98	1.000
^{238}U	TAIL	< 0.98	1.000

STRUC-I classifies all these isotopes by their $\bar{\rho}$ profiles under α or α_s deformation (e.g. ^{48}Ca TYPE III-Fr, ^{150}Nd TYPE III-Fr, ^{208}Pb TYPE I-calm). It does not detect the FULL/TAIL bifurcation: ^{48}Ca and the FULL isotopes share comparable $\bar{\rho}$ values. STRUC-PERC-I reveals the internal structural differentiation within the nuclear domain. This is the Realizability Refinement Theorem (Theorem 7.1) in operation.

11.5 The Biological Case: Immediate Connectivity

The biological corpus (QT45 ribozyme fitness landscape, 7 runs) returns FULL percolation with $\kappa_{\text{conn}} = 0.42\text{--}2.00$ across all runs—the lowest connectivity threshold of any domain in the corpus. This means the fitness landscape gap structure is the most locally homogeneous in Δ -space of all tested systems.

At $\bar{\rho}$ values overlapping the lower nuclear range ($\bar{\rho} \approx 0.19\text{--}0.30$), biological ladders connect at $\kappa_{\text{conn}} \leq 2$ while nuclear ladders connect at $\kappa_{\text{conn}} = 10^4\text{--}10^5$. This is a factor of $10^4\text{--}10^5$ difference in connectivity at comparable pressure—a direct empirical demonstration of Theorem 5.1.

The biological result extends the substrate-independence finding of [1]: not only does the admissibility constraint hold across physical and biological domains, but the realizability coordinate also registers a distinct, biologically characteristic value—immediate connectivity—that differentiates living-matter fitness landscapes from physical spectral systems at the same admissibility pressure.

11.6 Structural Phase Plane

Figure 1 displays the cross-instrument corpus in the $(\bar{\rho}, \kappa_{\text{conn}})$ coordinate plane. The horizontal axis is κ_{conn} on a logarithmic scale; systems without a finite κ_{conn} (TAIL and unconnected GIANT) are placed in the shaded “no connection” zone at the right margin. The vertical axis is structural pressure $\bar{\rho}$. Colour encodes joint structural state (Definition 8.3); horizontal shading marks the four admissibility pressure zones. The cross-hatched upper-right corner is the empirically forbidden (high $\bar{\rho}$, HARD) region (Theorem 9.1).

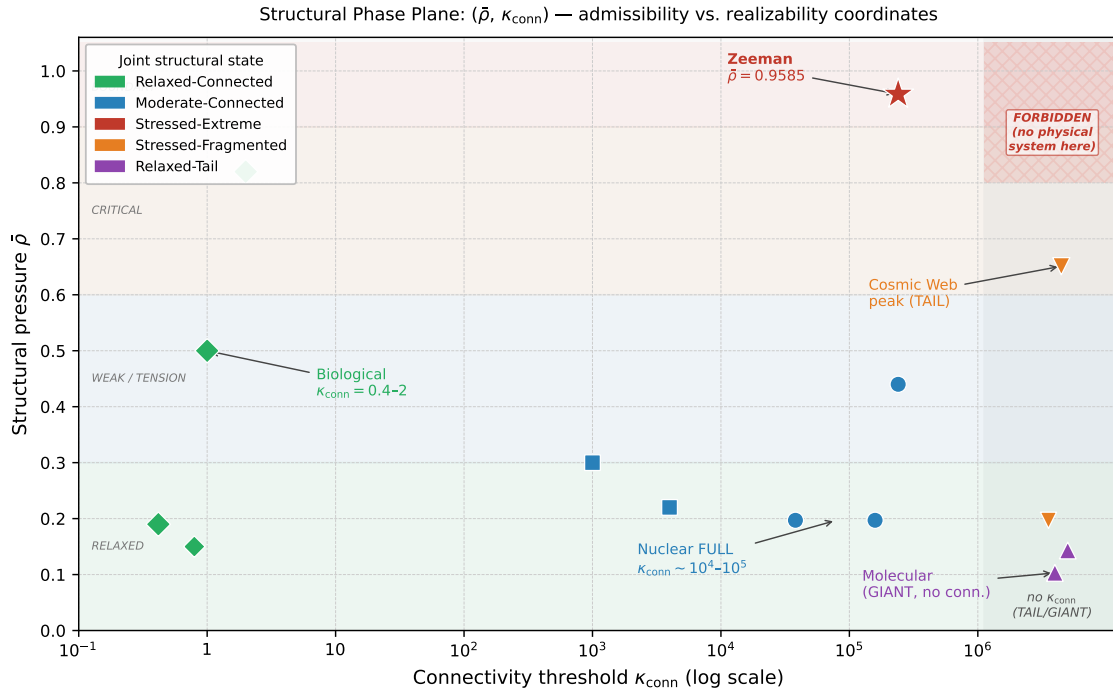


Figure 1: Structural phase plane $(\bar{\rho}, \kappa_{\text{conn}})$. The Zeeman domain (red star, upper right of the connected region) is the clearest demonstration of coordinate independence: maximum admissibility pressure with extreme connectivity delay. Biological ladders (green diamonds) occupy the left column at all pressure levels: low κ_{conn} regardless of $\bar{\rho}$. Nuclear FULL ladders (blue circles) cluster at moderate $\bar{\rho}$ and $\kappa_{\text{conn}} \sim 10^4\text{--}10^5$. TAIL and unconnected GIANT domains (right shaded zone) include molecular ladders (purple), nuclear TAIL isotopes (orange down-triangle), and cosmic web peak (orange). The cross-hatched upper-right region has no physical occupants, grounding the Forbidden State Theorem 9.1.

11.7 Instrument Consistency and the TiO_2 Exception

Zero physical contradictions arise between the two instruments across the 10 shared domains. Where STRUC-I classifies a system as Stable Structure, STRUC-PERC-I returns FULL or GIANT. Where STRUC-I finds Boundary-Stabilised, STRUC-PERC-I returns FULL at large κ_{conn} or TAIL.

The single HARD_FRAGMENTATION result (TiO_2 raw density-of-states, $\text{GR} = 0.833$) is a representation-sensitivity finding. STRUC-I evaluates TiO_2 as a crystallographic phase chain (rutile/anatase/brookite polymorphs, $n = 3$, $\bar{\rho} = 0.033$, FULL at $\kappa_{\text{conn}} = 681$). STRUC-PERC-I finds HARD only when applied to the raw density-of-states ladder—a different representation of the same material. The HARD result signals that this particular ladder representation is not admissible as a structural object; the physical crystal is not in the HARD class. This is a finding about representation sensitivity, not about the physical system.

12 Interpretive Consequences

The dual-layer theory generates four principal interpretive consequences.

Proposition 12.1 (Selection \neq Organisation). *Structural selection (the USL admissibility filter Σ) and structural organisation (the realizability coordinate \mathcal{R}) are independent operations on configuration space. Selection determines which configurations can exist as persistent structures; organisation determines how those structures are internally connected. Knowing that a configuration is selected ($\Sigma(S) = 1$) provides no information about its realizability class $\mathcal{C}(S)$ or connectivity threshold $\kappa_{\text{conn}}(S)$.*

Proof sketch. Immediate from Theorem 6.1: the realizability coordinate $\mathcal{R}(S)$ is not determined by $\bar{\rho}(S) = \bar{A}_\kappa(S)$, which is itself the primary output of the selection filter Σ . Since Σ acts by evaluating admissibility, and admissibility does not determine realizability, Σ and \mathcal{R} are independent. \square

Remark 12.2. Proposition 12.1 is the deepest consequence of the dual-layer theory. It identifies the specific logical gap between the Foundations theory (selection) and the realizability layer (organisation): they are not merely at different levels of the hierarchy—they are genuinely independent operations on the same space of admissible configurations.

12.1 Admissibility Is Necessary But Not Sufficient for Structural Organisation

The USL establishes that persistent configurations must be admissible. The Percolative Realizability Layer establishes that admissibility is not sufficient to determine *how* a configuration is internally organised. Two equally admissible systems can be organised entirely differently at the gap-connectivity level.

This shifts the scientific question from “does the system satisfy the bound?” to “how does the system realise its admissibility?” The second question is answered by the realizability coordinate.

12.2 Boundary Systems Are Dual-Tension States

Under the Foundations theory, boundary-adjacent systems are characterised by high structural pressure $\bar{\rho} \rightarrow 1$ and maximal sensitivity to operator deformation. The dual-layer theory adds a second characterisation: boundary-adjacent systems are also constrained in their realizability. The Forbidden State Theorem (Theorem 9.1) shows that high-pressure systems cannot be in the HARD class; the Zeeman case shows that they can achieve FULL percolation only at extreme connectivity delay.

A boundary-adjacent system is therefore in a *dual-tension state*: its admissibility coordinate approaches the ceiling of \mathcal{M}_{adm} (high pressure from the inversion direction) while its realizability coordinate approaches the ceiling of connectivity delay (full but late percolation from the gap-distance direction). Both tensions are manifestations of the same physical mechanism—the extremal gap structure of the system—but they are measured by instruments probing independent structural coordinates.

12.3 Structural Regimes Require the Two-Component State

The regime map of [1] (Ultra-Stable Interior, Weak Persistence, Boundary-Stabilised, Boundary-Adjacent) is a one-dimensional classification in $\bar{\rho}$. The dual-layer theory requires a two-dimensional regime map in $(\bar{\rho}, \mathcal{R})$. The five-state taxonomy of Definition 8.3 provides the first-order form of this two-dimensional map. It distinguishes, for example, Moderate-Connected nuclear systems (medium $\bar{\rho}$, FULL, moderate κ_{conn}) from Relaxed-Tail molecular systems (low $\bar{\rho}$, GIANT, no κ_{conn}) that the admissibility taxonomy places in the same zone.

12.4 The Geometry of \mathcal{M}_{adm} Is Not Captured by Pressure Alone

The Coordinate Independence Theorem (Theorem 6.1) and Remark 6.2 establish that \mathcal{M}_{adm} admits at least a two-dimensional coordinate chart. It admits an internal stratification along the realizability axis. A full geometric description of \mathcal{M}_{adm} requires both the admissibility coordinate $(\bar{\rho}, A_k^{\text{min}})$ and the realizability coordinate $(\mathcal{C}, \kappa_{\text{conn}})$. The manifold’s geometry is therefore richer than the Foundations framework captures, and the dual-layer theory provides the tools to describe it.

13 Discussion and Open Questions

13.1 Relation to the PRP

The Percolative Realizability Principle [2] establishes the necessary direction: HARD-class fragmentation implies a USL-violating deformation exists. The present paper uses STRUCPERC-I to classify the realizability of admissible configurations, and identifies the non-reducibility of that classification to the admissibility measure.

The PRP is therefore a statement about the boundary between \mathcal{M}_{adm} and its complement: non-percolation is a structural signature of impending USL violation. The present paper is a statement about the interior of \mathcal{M}_{adm} : even among admissible configurations, realizability varies independently. The two analyses are complementary: one maps the edge of \mathcal{M}_{adm} ; the other maps its interior.

13.2 The Sufficient Direction

The sufficient direction of the PRP (percolation implies admissibility for all deformations) remains open. If confirmed, it would elevate the realizability coordinate to a complete characterisation of admissibility: a configuration is admissible if and only if it percolates. In that case, the two coordinates would not be independent—realizability would determine admissibility.

The current evidence (zero violations among 48 FULL and 23 GIANT cases) is consistent with the sufficient direction but does not prove it. The dual-layer theory does not depend on the sufficient direction: even if percolation implies admissibility, it does not follow that κ_{conn} determines $\bar{\rho}$. The coordinate independence of the two observables is a statement about the coordinates themselves, not about the admissibility boundary.

13.3 Open Questions

The dual-layer theory generates the following open mathematical questions.

1. **Characterisation of the forbidden state.** Theorem 9.1 is corpus-relative. Is there a mathematical proof that $\bar{\rho} \rightarrow 1$ implies $\mathcal{C} \neq \text{HARD}$? Such a proof would require showing that the gap structure generating high inversion pressure must also generate eventual global connectivity.
2. **Dimension of the two-coordinate space.** The current corpus spans a 10-domain slice of the full $(\bar{\rho}, \mathcal{R})$ plane. Is the distribution of physical systems in this plane constrained to a lower-dimensional manifold, or does it fill the available two-dimensional space?
3. **Realizability under operator deformation.** The admissibility coordinate $\bar{\rho}$ responds to operator deformations $(\alpha, \mu, \alpha_s, \alpha_G)$ in domain-characteristic ways (the four-column programme of [1]). How does the realizability coordinate \mathcal{R} respond to the same deformations? Does the realizability class change under constant sweeps, or is it invariant? This is an empirical question accessible to STRUC-PERC-I.
4. **Biological realizability under deformation.** The biological corpus has not been subjected to operator deformations (there is no direct analogue of the μ -sweep for fitness landscapes). Is the immediate connectivity ($\kappa_{\text{conn}} \leq 2$) of biological ladders invariant under structural perturbations of the fitness landscape, or does it depend on the specific mutational regime?
5. **Extension to information-theoretic sequences.** The substrate-independence result of [1] motivates testing whether information-theoretic and computational-complexity ladders are admissible. The dual-layer theory adds a second question: what is the realizability class of such sequences? Are they Relaxed-Connected (like biological ladders) or Relaxed-Tail (like molecular ladders)?
6. **Topology of the two-coordinate manifold.** The pair $(\bar{\rho}, \mathcal{R})$ defines a two-dimensional coordinate chart on \mathcal{M}_{adm} . The global topology of this chart—whether it is simply connected, whether it has holes or boundaries in the \mathcal{R} direction—is unknown and constitutes the central geometric open problem of the dual-layer theory.

14 Conclusion

14.1 What Has Been Established

The cross-instrument analysis (STRUC-I v1.0.4 \times STRUC-PERC-I v2.4.0, 10 shared domains, zero physical contradictions) establishes the following:

Dual Observability. Every admissible configuration admits two independent structural projections. The admissibility projection (structural pressure $\bar{\rho}$, admissibility score A_{κ}^{\min}) measures inversion budget usage. The realizability projection (percolation class \mathcal{C} , connectivity threshold κ_{conn}) measures gap-graph connectivity. Neither determines the other.

Non-Equivalence. Equal admissibility does not imply equal realizability. Nuclear, molecular, and biological ladders sharing structural pressure zones differ by factors of 10^4 – 10^5 in κ_{conn} .

Coordinate Independence. The two coordinates are empirically independent on \mathcal{M}_{adm} . The Zeeman domain, with the highest pressure and highest connectivity delay in the corpus, provides the sharpest demonstration.

Refinement. The five-state joint taxonomy (Relaxed-Connected, Moderate-Connected, Relaxed-Tail, Stressed-Extreme, Stressed-Fragmented) is strictly more discriminating than either instrument’s taxonomy alone.

Forbidden State. No physical system occupies the (high $\bar{\rho}$, HARD) cell. The only HARD result is a representation-sensitivity finding on a non-physical TiO_2 ladder. The pattern *suggests* a structural incompatibility between extreme inversion pressure and persistent fragmentation, but is corpus-relative and does not assert logical necessity.

Layered Structure. Realizability sits strictly between admissibility and dynamics in the logical hierarchy. It is defined within \mathcal{M}_{adm} and presupposes admissibility; it does not determine dynamical behaviour.

Selection \neq Organisation. The selection filter Σ and the realizability coordinate \mathcal{R} are independent operations: knowing that a configuration is admissible ($\Sigma(S) = 1$) gives no information about its connectivity regime $\mathcal{C}(S)$ or threshold $\kappa_{\text{conn}}(S)$.

14.2 What This Changes

The dual-layer theory changes the status of three components of the structural framework.

The admissibility manifold \mathcal{M}_{adm} admits at least two coordinates. Its internal structure requires both $(\bar{\rho}, A_{\kappa}^{\min})$ and $(\mathcal{C}, \kappa_{\text{conn}})$. The structural pressure $\bar{\rho}$ is a proximity measure toward the boundary $\partial\mathcal{M}_{\text{adm}}$ in the inversion direction; the connectivity threshold κ_{conn} is an independent structural coordinate measuring depth of organisational integration. Whether the two coordinates span a full product structure on \mathcal{M}_{adm} is an open mathematical question.

The selection principle is not the end of the story. Admissibility ($\Sigma(S) = 1$) determines that S can persist. Realizability ($\mathcal{C}(S), \kappa_{\text{conn}}(S)$) determines how S is internally connected as a persistent object. The selection principle constrains existence; the realizability principle constrains organisation. These are independent constraints, as Proposition 12.1 makes precise.

Null results in realizability have content. TAIL and GIANT classifications are not failures; they are positive measurements of a system’s internal connectivity regime. A GIANT result means the bulk of the gap structure is globally connected while an outlier tail remains isolated—a finding about the internal architecture of the system, not a shortcoming of the measurement.

14.3 The Central Shift

The single-inequality framework asked: *does the system satisfy the bound?*

The dual-layer theory asks: *how does the system realise its admissibility?*

The first question is answered by STRUC-I alone. The second requires both instruments. The second question is the deeper one: it places admissible configurations in a two-dimensional structural coordinate system and reveals that physical systems occupy a structured, non-uniform landscape within \mathcal{M}_{adm} that the admissibility coordinate alone cannot characterise.

Synthesis. The Universal Structural Law defines the admissible domain \mathcal{M}_{adm} of relational configurations. The Percolative Realizability Principle defines the internal organisation of \mathcal{M}_{adm} . Together they form a dual-layer theory of structural science in which admissibility bounds existence and realizability governs structural connectivity. Physical systems do not merely satisfy a bound; they inhabit a two-dimensional structural state space, and the geometry of that space is measurable, domain-characteristic, and not reducible to either coordinate alone.

Admissibility answers whether a structure can exist.

*Realizability answers **how** it exists.*

A Proof of the Dual Observability Theorem

This appendix gives the complete two-step proof of Theorem 4.1.

A.1 Step 1: Logical Non-Reducibility

Admissibility projection (STRUC-I coordinate). For a ladder L with gaps $\Delta_i = x_{i+1} - x_i$ and median gap $\tilde{\Delta}$, set $\varepsilon = \kappa \tilde{\Delta}$. Define the ε -persistence set $P_\varepsilon(L) = \{(i, j) : x_j - x_i > \varepsilon\}$. Then:

$$\bar{\rho}(S) = \frac{1}{|\mathcal{K}|} \sum_{\kappa \in \mathcal{K}} A_\kappa(S, c), \quad A_\kappa(S, c) = \frac{\text{inv}(P_\varepsilon; L)}{\nu(V_\varepsilon(L))},$$

where $\text{inv}(P_\varepsilon; L)$ counts order-inverting pairs and $\nu(V_\varepsilon(L)) = |P_\varepsilon(L)|$ is the admissible inversion capacity. The scalars $\bar{\rho}$ and A_κ^{\min} are functions of these inversion counts alone.

Realizability projection (STRUC-PERC-I coordinate). The vulnerability graph $G_\kappa(L) = (V, E_\kappa)$ has vertex set $V = \{1, \dots, n-1\}$ indexing gaps Δ_i and edge set

$$(i, j) \in E_\kappa \iff |\Delta_i - \Delta_j| \leq \varepsilon = \kappa \tilde{\Delta}.$$

The realizability class $\mathcal{C}(S) \in \{\text{FULL}, \text{GIANT}, \text{TAIL}, \text{HARD}\}$ and connectivity threshold $\kappa_{\text{conn}}(S)$ are connected-component invariants of $G_\kappa(L)$ across the scale grid \mathcal{K} .

Non-reducibility. There is no algebraic identity or functional relation equating the inversion-count scalars $\bar{\rho}$, A_κ^{\min} with the graph-connectivity invariants \mathcal{C} , κ_{conn} : the former depend only on the number of inverting pairs among elements of P_ε ; the latter depend on which gap-magnitude pairs fall within exchange distance ε in the gap-distance graph. A ladder that has many inverting pairs need not have a fragmented gap graph, and a ladder with a connected gap graph need not have any particular inversion count. Hence the projections are logically distinct; independence is established empirically in Step 2.

A.2 Step 2: Empirical Coordinate Independence

The cross-instrument corpus (5,233 STRUC-I runs \times 81 STRUC-PERC-I runs, 10 shared domains) establishes that neither coordinate determines the other.

Counterexample set 1 (equal $\bar{\rho}$, different realizability).

- Nuclear domain (ENSDF, 14 isotopes): $\bar{\rho} \approx 0.197$ (RELAXED zone). Ten isotopes: FULL at $\kappa_{\text{conn}} = 3.8 \times 10^4$ – 4.2×10^5 . Four isotopes (^{48}Ca , ^{100}Mo , ^{150}Nd , ^{238}U): TAIL (tail dominance = 1.000, gap ratios up to 2×10^{18}).
- Molecular domain (HITRAN): $\bar{\rho} = 0.103$ (also RELAXED) \rightarrow GIANT, no κ_{conn} .

Thus $\bar{\rho} \approx 0.10$ – 0.20 spans FULL, TAIL, and GIANT simultaneously.

Counterexample set 2 (overlapping $\bar{\rho}$, extreme κ_{conn} difference).

- Biological domain (QT45 ribozyme, 7 runs): $\bar{\rho} \in [0.188, 0.819]$ \rightarrow FULL at $\kappa_{\text{conn}} = 0.42$ – 2.00 (lowest in corpus).
- Nuclear domain at comparable $\bar{\rho} \approx 0.19$ – 0.30 : FULL/TAIL at $\kappa_{\text{conn}} \sim 10^4$ – 10^5 .

Factor 10^4 – 10^5 difference in κ_{conn} at overlapping pressure.

Counterexample set 3 (same realizability class, wide $\bar{\rho}$ range).

- FULL class: $\bar{\rho} = 0.086$ (atmosphere) to $\bar{\rho} = 0.9585$ (Zeeman), factor 11.
- GIANT class: $\bar{\rho} = 0.103$ (molecular) to $\bar{\rho} \approx 0.65$ (cosmic web peak).
- TAIL class: appears at both low and elevated pressure.

Sharpest single instance — Zeeman domain. $\bar{\rho} = 0.9585 \pm 0.00004$ (CRITICAL zone, 4.15% margin to violation) combined with FULL percolation at $\kappa_{\text{conn}} = 2$ – 4×10^5 (most extreme connectivity delay in the corpus). Maximum inversion pressure and maximum connectivity delay coexist in the same physical system. Neither measurement predicts the other.

Conclusion. Since the corpus contains configurations with identical $\bar{\rho}$ but different \mathcal{C} and κ_{conn} (counterexample sets 1–2), and configurations with identical \mathcal{C} spanning a wide range of $\bar{\rho}$ (counterexample set 3), no functional relation $\mathcal{R} = f(\bar{\rho})$ or $\bar{\rho} = g(\mathcal{R})$ holds. The coordinates are empirically independent. Combined with Step 1, this establishes that every admissible configuration S requires the two-component structural state $\mathcal{S}(S) = (\bar{\rho}(S), \mathcal{R}(S))$ for complete characterisation, proving Theorem 4.1.

Corollaries (immediate consequences).

- Non-Equivalence Theorem 5.1: there exist S_1, S_2 with $\bar{\rho}(S_1) = \bar{\rho}(S_2)$ but $\mathcal{R}(S_1) \neq \mathcal{R}(S_2)$.
- Coordinate Independence Theorem 6.1: admissibility and realizability define independent coordinates on \mathcal{M}_{adm} .
- Realizability Refinement Theorem 7.1: realizability induces a strictly finer partition of \mathcal{M}_{adm} than admissibility alone.
- Forbidden State Theorem 9.1: no physical system occupies $(\bar{\rho} \rightarrow 1, \mathcal{C} = \text{HARD})$; the single HARD case is representation-dependent.

B Formal Derivation of the Realizability Classes

We derive the four realizability classes rigorously from the vulnerability graph construction and the revised percolation conditions of the PRP [2] (Definition 9). The derivation shows that the classes form an exhaustive and mutually exclusive partition of all ladders based on their multi-scale connectivity structure, independent of the admissibility coordinate $\bar{\rho}$.

B.1 Vulnerability Graph (Foundation)

Let $L = (x_1 \leq x_2 \leq \dots \leq x_n)$ be a ladder ($n \geq 2$) with gap vector $\Delta = (\Delta_1, \dots, \Delta_{n-1})$, $\Delta_i = x_{i+1} - x_i \geq 0$, median gap $\tilde{\Delta} = \text{median}(\Delta)$, and scale domain $\mathcal{K} = \{\kappa_1 < \dots < \kappa_m\} \subset (0, 1]$ (standard: 17-point grid in STRUC-I; 40-point grid with Monte Carlo sampling in STRUC-PERC-I).

For each scale $\kappa \in \mathcal{K}$, the vulnerability graph is $G_\kappa(L) = (V, E_\kappa)$ with $V = \{1, \dots, n-1\}$ and edge predicate $(i, j) \in E_\kappa \iff |\Delta_i - \Delta_j| \leq \varepsilon = \kappa \tilde{\Delta}$.

Remark B.1 (Nestedness). Edge sets are nested: $\kappa_1 < \kappa_2 \Rightarrow E_{\kappa_1} \subseteq E_{\kappa_2}$. Hence connected components only merge (never split) as κ increases.

B.2 Giant Ratio and Dominant Backbone

For each κ , let $C_{\kappa, \text{max}}$ be a largest connected component of $G_\kappa(L)$. Define the *giant ratio*

$$\text{GR}(\kappa) = \frac{|C_{\kappa, \text{max}}|}{|V|}.$$

A *dominant backbone* at scale κ is any connected component C_κ with $|C_\kappa| \geq \text{GR}_{\text{thresh}} \cdot |V|$ for a fixed threshold $\text{GR}_{\text{thresh}} \in (0, 1]$.

B.3 Derivation of the Four Classes

The classes are the natural exhaustive partition induced by the revised percolation condition of the PRP [2] (Definition 9).

FULL class (complete connectivity). L is scale-percolating with $\text{GR}_{\text{thresh}} = 1$, i.e. $|C_{\kappa_{\text{max}}, \text{max}}| = |V|$: no isolated vertices at the largest scale. *Derivation:* set $\text{GR}_{\text{thresh}} = 1$ in Condition 4; the dominant backbone must include every vertex.

GIANT class (near-complete connectivity). L is scale-percolating with $\text{GR}_{\text{thresh}} < 1$ and $\text{GR}(\kappa_{\text{max}}) \geq \text{GR}_{\text{thresh}}$ (typically $\text{GR}_{\text{thresh}} \approx 0.90$ in STRUC-PERC-I v2.4.0). *Derivation:* Conditions 1–3 hold for the backbone; Condition 4 allows a negligible isolated tail $V \setminus C_{\kappa_{\text{max}}}$ of size $< (1 - \text{GR}_{\text{thresh}})|V|$.

TAIL class (non-percolating, large backbone with extreme outliers). L fails scale-percolation because Condition 4 cannot be satisfied within the tested \mathcal{K} : despite a large backbone, one or more extreme outlier gaps with ratios $\gg 10^6$ (up to $\sim 2 \times 10^{18}$ in the nuclear corpus) remain permanently isolated, preventing $\text{GR}(\kappa_{\text{max}}) \geq \text{GR}_{\text{thresh}}$. *Derivation:* Conditions 1–3 hold for a dominant component; Condition 4 fails because outliers prevent full merger. Tail dominance = 1.000 is the operational signature.

HARD class (severe persistent fragmentation). L fails scale-percolation because Conditions 1–3 fail persistently: the graph remains multi-component with $\text{GR}(\kappa) < \text{GR}_{\text{thresh}}$ at all scales in \mathcal{K} . *Derivation:* no family $\{C_\kappa\}$ satisfies the full set of conditions; the graph exhibits global isolation of components across the entire scale range. HARD is the only class that triggers the restricted necessary direction of the revised PRP (Theorem 1, [2]): it implies the existence of a USL-violating deformation.

B.4 Exhaustiveness and Mutual Exclusivity

Every ladder either satisfies the four conditions of Definition 9 of [2] (for some $\text{GR}_{\text{thresh}}$) or it does not:

- Satisfies them with $\text{GR}_{\text{thresh}} = 1 \rightarrow \text{FULL}$.
- Satisfies them with $\text{GR}_{\text{thresh}} < 1$ and $\text{GR}(\kappa_{\text{max}}) \geq \text{GR}_{\text{thresh}} \rightarrow \text{GIANT}$.
- Fails only Condition 4 (large backbone with permanent outliers) $\rightarrow \text{TAIL}$.
- Fails Conditions 1–3 severely (no dominant backbone at any scale) $\rightarrow \text{HARD}$.

No overlap is possible, and every ladder falls into exactly one class. The partition is therefore exhaustive and mutually exclusive.

Remark B.2 ($\text{GR}_{\text{thresh}}$ invariance). The partition is invariant for fixed $\text{GR}_{\text{thresh}}$: the class boundaries (FULL/GIANT and GIANT/TAIL) depend on the chosen threshold, but exhaustiveness and mutual exclusivity hold for any fixed value. Changing $\text{GR}_{\text{thresh}}$ induces a controlled reclassification at the GIANT/TAIL boundary without affecting the logical structure of the partition or the FULL and HARD classes. In particular: (i) FULL and HARD are defined by $\text{GR}_{\text{thresh}} = 1$ and $\text{GR}_{\text{thresh}}$ -failure, respectively, and are robust to moderate threshold variation; (ii) the GIANT/TAIL boundary is the threshold-sensitive

interface, and the STRUC-PERC-I implementation value $\text{GR}_{\text{thresh}} \approx 0.90$ is chosen to match the empirical separation between the outlier-free bulk and the extreme-ratio tails in the physical corpus.

B.5 Link to Dual Observability

The four realizability classes define the realizability coordinate $\mathcal{R}(S) = (\mathcal{C}(S), \kappa_{\text{conn}}(S))$, where $\kappa_{\text{conn}}(S)$ is the smallest κ at which FULL or GIANT is first achieved (undefined for TAIL/HARD). This coordinate is independent of the admissibility coordinate $\bar{\rho}(S)$ (Theorem 4.1), as proven by the corpus: equal $\bar{\rho}$ spans multiple classes, and each class spans wide ranges of $\bar{\rho}$. The classes therefore constitute the second structural layer (realizability) on the admissibility manifold \mathcal{M}_{adm} , lying strictly between admissibility and dynamics (Theorem 10.1).

Implementation note. In STRUC-PERC-I v2.4.0: $\text{GR}_{\text{thresh}} \approx 0.90$; $\varepsilon = \kappa \cdot \text{IQR}(\Delta)$ with fallback to median; MAX_WINDOW = 64; adaptive κ -extension up to 10^6 .

References

- [1] UNNS Substrate Research Program. *Foundations of the UNNS Substrate: From Universal Admissibility to Structural Regime Theory*. Foundation Document, Intermediate Stage, 2026.
- [2] UNNS Substrate Research Program. *The Percolative Realizability Principle: Admissibility as Global Connectivity of the Vulnerability Graph*. Working Manuscript, 2026.
- [3] UNNS Substrate Research Program. *Cross-Instrument Corpus Analysis: STRUC-I v1.0.4 × STRUC-PERC-I v2.4.0*. Internal Report, 2026-04-06.
- [4] UNNS Substrate Research Program. *STRUC-PERC Corpus Analysis: Full Pairwise Vulnerability Graph, 81 Runs across 14 Domains*. Internal Report, 2026-04-05.
- [5] UNNS Substrate Research Program. *Admissibility in Living Matter: Structural Analysis of the QT45 Ribozyme Fitness Landscape*. <https://unns.tech/labs/admissibility-in-living-matter>, March 2026.